

# The Monoacylglycerol Lipase Inhibitor JZL184 and ARDS: Differential Effects in Direct and Indirect Rat Models

Yusuf Elma<sup>1</sup>, Emine Yilmaz Can<sup>1\*</sup>, Meryem Akpolat Ferah<sup>2</sup> and Mete Kececi<sup>2</sup>

<sup>1</sup>Department of Medical Pharmacology, Faculty of Medicine, Zonguldak Bulent Ecevit University, Zonguldak, Kozlu, 67600, Turkey

<sup>2</sup>Department of Histology and Embryology, Faculty of Medicine, Zonguldak Bulent Ecevit University, Zonguldak, Kozlu, 67600, Turkey

## \*Corresponding Author

Emine Yilmaz Can, Department of Medical Pharmacology, Faculty of Medicine, Zonguldak Bulent Ecevit University, Zonguldak, Kozlu, Turkey.

Submitted: 2024, Nov 22; Accepted: 2024, Dec 16; Published: 2024, Dec 31

**Citation:** Elma, Y., Yilmaz Can, E., Akpolat Ferah, M., Kececi, M. (2024). The Monoacylglycerol Lipase Inhibitor JZL184 and ARDS: Differential Effects in Direct and Indirect Rat Models. *J Anesth Pain Med*, 9(4), 01-08.

## Abstract

**Purpose:** Acute respiratory distress syndrome (ARDS) leads to high morbidity and mortality, with limited pharmacological treatments and a reliance on supportive therapies. Recent evidence suggests cannabinoids may offer protective and therapeutic benefits against tissue damage, including lung pathologies. While cannabinoids' positive impacts on lung pathologies are known, their specific effects on ARDS mechanisms have not been thoroughly examined. The study purposes to explore the protective effects of cannabinoids on lung injury in direct and indirect ARDS models, focusing on differences in pathophysiological mechanisms.

**Methods:** Rats received lipopolysaccharide (LPS, 5 mg/kg, intratracheally) for direct models or alpha-naphthylthiourea (ANTU, 10 mg/kg, intraperitoneally) for indirect models. Endocannabinoid degrading enzyme, MAGL inhibitor JZL184 (10 mg/kg, i.p.) was administered 30 min before LPS or ANTU. After 24 hours of LPS and 4 hours of ANTU applications lung tissue samples were collected.

**Results:** In the LPS group, significant epithelial damage and intense NF- $\kappa$ B and caspase-3 staining around the bronchiolar epithelium were observed, with JZL184 effectively reducing inflammation and these markers in the area. In the ANTU group, the damage was more focused on the endothelium with similar increases in NF- $\kappa$ B and caspase-3 staining in the alveolar walls, where JZL184 also decreased inflammation and markers intensity. Overall, JZL184 showed a protective effect against inflammation, apoptosis, and tissue damage in lung injuries, highlighting the therapeutic potential of MAGL inhibition in ARDS treatment, with variations in effects depending on the injury model.

**Conclusion:** MAGL inhibition showed model-specific benefits against ARDS-related inflammation, apoptosis, and tissue damage, highlighting its therapeutic potential.

**Keywords:** ARDS, ANTU, LPS, Cannabinoid, MAGL, JZL184

## 1. Introduction

Acute respiratory distress syndrome (ARDS) is characterized by noncardiac pulmonary edema, increased alveolo-capillary permeability, inflammation, fibrosis, hypoxemia unresponsive to oxygen therapy, decreased lung compliance, decreased functional residual capacity, and diffuse chest radiograph infiltrates. ARDS is caused by direct or indirect lung damage from causes such as sepsis, pneumonia, trauma, burns, lung transplants, fat embolism, smoke inhalation, cardiopulmonary bypass, and acute pancreatitis

[1,2]. Despite its prevalence, treatment of ARDS has remained largely symptomatic and pharmacotherapy has not passed the experimental stage in this regard [3,4]. As clinical research in this area faces challenges, intensive experimental studies are needed to overcome this treatment gap.

Extensive clinical studies have highlighted the significant role of cannabinoids (CB) in various medical conditions, including inflammatory, autoimmune, cardiovascular, gastrointestinal,

liver, kidney, lung diseases, neurodegenerative and psychiatric disorders, chronic pain, and cancer [5-10]. These findings have led to planned clinical trials to assess the efficacy and safety of phytocannabinoids. However, the use of cannabinoids in medicine is constrained by their neuropsychiatric effects. The discovery of delta-9 tetrahydrocannabinol (THC) helped clarify the cannabinoid system's receptors, effects, and side effects. THC is psychoactive, whereas cannabidiol (CBD) is not and is considered safer due to the lack of euphoric effects [6,11]. Endocannabinoids like anandamide (AEA) and 2-arachidonoylglycerol (2-AG) are naturally produced and regulated by enzymes such as fatty acid amide hydrolase (FAAH) and monoacylglycerol lipase (MAGL), playing crucial roles in the endocannabinoid system's function [12,13].

Alpha-naphthylthiourea (ANTU), a rodenticide, induces indirect lung injury by causing pulmonary edema and pleural effusion [14-23]. Lipopolysaccharide (LPS), found in gram-negative bacterial membranes, leads to direct lung injury through acute

inflammation when administered intratracheally [24]. Our study used ANTU and LPS to create indirect and direct ARDS models, respectively, aiming to explore the distinct pathophysiological mechanisms of lung injury, assess the protective potential of the MAGL inhibitor JZL184, and identify model-specific effects.

## 2. Materials and Methods

### 2.1. Animals

50 male Wistar albino rats (200-250 g, 3-4 months old) from Zonguldak Bulent Ecevit University animal laboratory were used. They were kept in standard conditions (22 ± 2 °C, 12/12 h light/dark cycle), with unlimited access to water and 21% protein pellet feeds.

### 2.2. Experimental Groups

Rats were randomly divided into 5 groups with equal numbers (n=10) (Table 1).

	Groups	Chemicals	Route of Application
1	Control	-	
2	ANTU (indirect pathology)	ANTU (10 mg/kg)	i.p.
3	LPS (direct pathology)	LPS (5 mg/kg)	intratracheal
4	ANTU+JZL184 (treatment)	ANTU (10 mg/kg) + JZL184 (10 mg/kg) 30 min before ANTU application	i.p./i.p.
5	LPS+JZL184 (treatment)	LPS (5 mg/kg) + JZL184 (10 mg/kg) 30 min before LPS application	intratracheal/i.p.

**Table 1: Experimental Groups**

### 2.3. ANTU (Indirect ARDS) Model

ANTU was suspended in olive oil (4 mg/ml) and given to rats at the dose of 10 mg/kg. After 4 hours, they were anesthetized with ketamine-xylazine (75 mg/kg i.p.-5 mg/kg intramuscular), then euthanized by abdominal aorta bleeding. Pleural effusion was collected and measured, and the lungs were removed, cleaned, and weighed [14-16,18-23].

### 2.4. Intratracheal LPS (Direct ARDS) Model

The neck areas of the animals were shaved under ketamine and xylazine anesthesia, were positioned supine, and a 1 cm incision was made along the midline to expose the trachea for intratracheal instillation of LPS dissolved in saline, administered at 5 mg/kg. Following the procedure, the animals were gently shaken in an upright position to facilitate the distribution of LPS within the lungs. To mitigate the risk of respiratory depression, animals were then placed in their cages at a 45-degree incline until they fully recovered from anesthesia. Twenty-four hours after the LPS administration, the animals were anesthetized and euthanized to assess the effects on the lungs. The chest was opened to remove the lungs, which were then cleaned, weighed, and analyzed in relation to the animal's body weight to standardize the results across all subjects. Key metrics for evaluating ARDS included the ratio of pleural effusion volume and lung weight to body weight. The amount of pleural effusion fluid (PE), pleural effusion/body weight (PE/BW) and lung weight/body weight (LW/BW) ratios were evaluated as indicators of ARDS.

### 2.5. Biochemical Examination - Detection of Reduced Glutathione (GSH) in Lung Tissue (mg/L)

The ELISA rat GSH kit (BT-Lab) was used for measuring GSH in lung tissue. The ELISA procedure was applied in a similar way as in our previous study [25].

### 2.6. Light Microscopic Procedures

Lung tissues were fixed in 10% formaldehyde for 48 hours and sectioned to 5 µm thickness from paraffin blocks. Sections were stained with hematoxylin-eosin following established methods [26]. Under a light microscope, tissues were assessed for edema, alveolar wall thickening, interstitial inflammation, vacuolization, macrophages, hemorrhage, perivascular enlargement, congestion, and bronchiolar inflammatory cells. Damage was scored from 0 (normal), 1 (mildly damaged), 2 (moderately damaged), and 3 (severely damaged).

### 2.7. Immunohistochemical Analyses

5 µm sections from paraffin blocks were placed on charged slides, deparaffinized, and antigen sites exposed in citrate buffer in a microwave. After cooling and PBS washes, sections were treated with 3% H<sub>2</sub>O<sub>2</sub> to block endogenous peroxidase and Ultra V block to prevent non-specific binding. Anti-caspase-3 and anti-NF-κB primary antibodies were applied, followed by biotinylated secondary antibody and streptavidin-peroxidase. DAB chromogen and hematoxylin were used for staining and counterstaining. Sections were kept humid to avoid background

staining and examined under a light microscope, using a Zeiss Axio Lab. A1 photomicroscope for imaging. Histological scoring (H score) assessed staining intensity, calculated by multiplying the percentage of stained cells by their density, with scoring done at x40 magnification across 20 fields per section for statistical analysis, following the formula  $H\text{-score} = \sum i \times P_i$ , where  $i$  is the density score and  $P_i$  is the cell percentage [27].

## 2.8. Chemicals

ANTU, LPS, and olive oil were purchased from Sigma-Aldrich (Missouri, USA), JZL184 from Santa Cruz Biotechnology (Texas, USA), ketamine from Pfizer (Ketalar 500 mg/10ml, USA), xylazine from Bioveta (Xylazinbio 2%, Czech Republic), and saline was 0.9% NaCl.

## 2.9. Statistical Analyses of Results

Statistical analyses were performed using Jamovi 2.3.21, with data presented as mean  $\pm$  SD. Normality was checked with Shapiro-Wilk test. For non-normal variables, Kruskal-Wallis test was used, followed by Mann-Whitney U with Bonferroni correction for subgroup analyses. Fisher-Freeman-Halton chi-square test assessed qualitative variables. A p-value  $< 0.05$  was deemed statistically significant.

## 3. Results

### 3.1. Control group (Healthy) Lungs

Hemorrhage, edema and pleural effusion were not detected in healthy rat lungs. Macroscopically, it has a light pink appearance (Figure 1A). Histopathological examination also shows normal-appearing lung tissue (Figure 4a).

### 3.2. Effect of ANTU on the Lung Tissue (Indirect Model)

In ANTU-treated rats, lungs were edematous and hemorrhagic (Fig. 1B, 1C) with significant increases in lung weight/body weight (LW/BW) and pleural effusion/body weight (PE/BW) ratios compared to controls (Fig. 2A-C). Non-hemorrhagic pleural effusion development was observed in ANTU group (Fig. 2B-C). Lung damage indicators were elevated in the ANTU group (Figs. 3B-G), with no inflammatory cells in bronchiolar lumens. There was a statistically significant increase in perivascular enlargement and congestion in the ANTU group compared to the control group ( $p < 0.001$ ). In Fig. 4b, hematoxylin-eosin staining revealed postcapillary venule congestion (asterisk in A and B), hemorrhage (arrow in A and B) into the adventitia of the adjacent mid-diameter vein, diffuse intra-alveolar and septal edema with vacuolization (asterisk in C), erythrocytes indicating intra-alveolar hemorrhage (asterisk in D), intra-alveolar macrophages (arrowhead in D) and inflammatory cell infiltrates in the alveolar wall (arrow in D). As shown in Fig. 3 (H and I) and Fig. 5, immunohistochemical analyses showed a significantly increased NF- $\kappa$ B and caspase-3 in the ANTU group's alveolar walls, indicating enhanced tissue damage.

### 3.3. Effect of LPS on the Lung Tissue (Direct Model)

In the LPS-treated group, lungs were notably hyperemic (Fig. 1D), with a significant increase in the lung weight/body weight (LW/

BW) ratio (Fig. 2A), but no pleural effusion observed (Fig. 2B). Lung damage parameters were significantly higher in the LPS group (Fig. 3B-G). There was a statistically significant increase in perivascular enlargement, congestion and inflammatory cells in the bronchiolar lumen in the LPS group compared to the control group ( $p < 0.001$ ). In Fig. 4c, hematoxylin-eosin staining showed dense vascular congestion (arrow in A) and alveolar wall thickening (asterisk in A), the presence of inflammatory cells in the bronchiolar lumen (asterisk in B), dilated adventitia of the small artery and diffuse inflammatory cells in peribronchiolar tissue (arrowhead in B), congestion in the small artery lumen (arrow in B), numerous erythrocyte crystalloids within the thickened alveolar wall (arrow in C) and the macrophages within the alveolar wall (arrowhead in C), desquamation areas in the bronchiolar epithelium (arrowhead in D), the presence of inflammatory cells in the bronchiolar lumen (asterisk in D). As shown in Fig. 3 (H and I) and Fig. 5, immunohistochemical analysis showed increased NF- $\kappa$ B and caspase-3 in the LPS group, particularly around the bronchiolar epithelium, indicating elevated tissue damage.

### 3.4. Effects of JZL184 on ANTU-induced Lung Injury

In the ANTU+JZL184 group, lungs showed less hemorrhage and edema than the ANTU group, with areas resembling healthy tissue. In addition, light pink areas similar to healthy lung tissue were observed (Fig. 1E). While LW/BW and PE/BW ratios, and pleural effusion, decreased compared to ANTU, these changes weren't statistically significant (Fig. 2A-C). Edema, inflammatory cell infiltration in the interstitium and perivascular enlargement were significantly reduced compared to the ANTU group (Fig. 3B, 3D,  $p < 0.001$ ). In Fig. 4d, hematoxylin-eosin staining showed thin-walled alveoli without edema, vein with slight perivascular enlargement (arrowhead in A), near-normal appearance lung tissue with mostly normal thickness but with slightly thickened alveolar walls in some areas (in B), near-normal appearance lung tissue with a limited area of intra-alveolar and septal edema (asterisk in C) and slight perivascular enlargement (arrowhead in C). As shown in Fig. 3 (H and I) and Fig. 5, immunohistochemical analyses revealed a statistically significant decrease in NF- $\kappa$ B and caspase-3 staining in the ANTU+JZL184 treatment group, especially in the alveolar wall tissue compared to the ANTU group.

### 3.5. Effects of JZL184 on LPS-induced Lung Injury

In the LPS+JZL184 group, lungs appeared macroscopically less hyperemic resembling healthy tissue and light pink areas similar to healthy lung tissue were observed (Fig. 1F). The LW/BW ratio did not significantly change from the LPS group (Fig. 2A), and no pleural effusion was observed (Fig. 2B). GSH levels significantly increased compared to LPS-treated lungs (Fig. 3A). Edema, perivascular enlargement, and bronchiolar inflammation were statistically significantly reduced (Fig. 3B,  $p < 0.001$ ). In Fig. 4e, hematoxylin-eosin staining showed normal-appearing alveoli with limited areas of slight wall thickening (in A), basal body line with cilia on the apical plasma membrane of ciliated cells in normal-appearing bronchiolar epithelium (arrowhead in B), normal-appearing alveoli with limited areas of slight wall thickening, mild vasocongestion (arrow in C) and normal-appearing bronchioles

(asterisk in C) with lumens free of inflammatory cells. As shown in Fig. 3 (H and I) and Fig. 5, immunohistochemical analysis indicated significant reductions in NF- $\kappa$ B and caspase-3 staining,

particularly in and around bronchiolar epithelium, suggesting reduced tissue damage with LPS+JZL184 treatment.

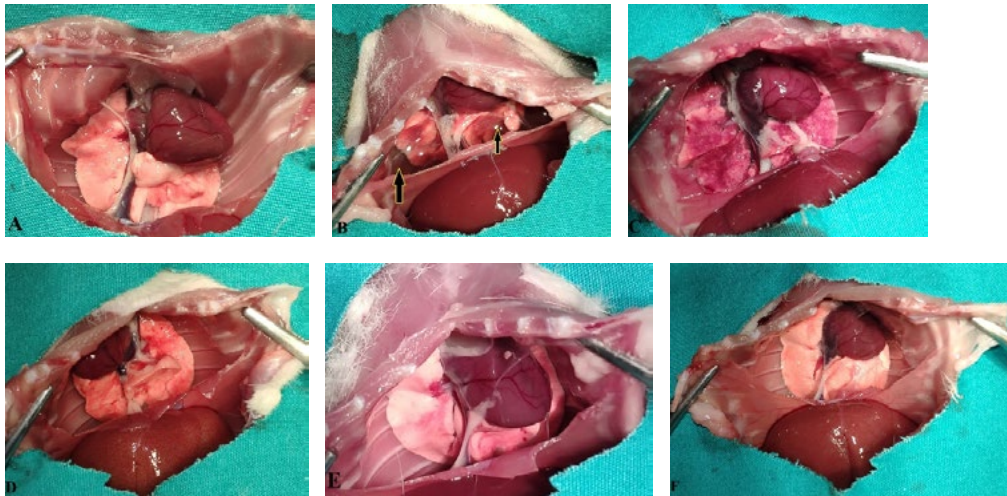


**Figure 1 A-F:** Macroscopic images of the lungs. A: Control, B and C: ANTU, D: LPS, E: ANTU+JZL184, F: LPS+JZL184. Edema fluid is shown with arrow in B

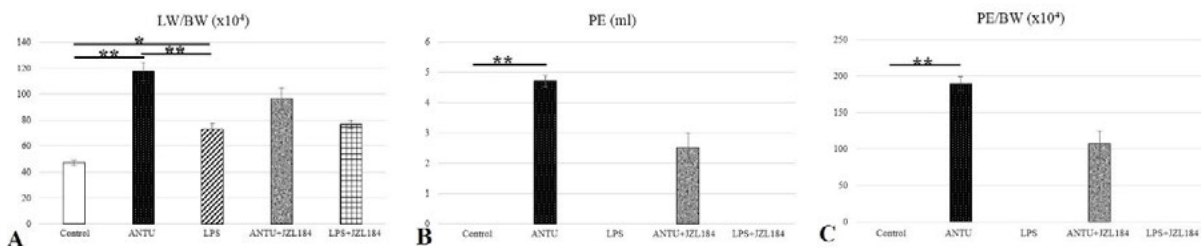


**Figure 2 A-C:** Calculated results of ARDS indicators induced by ANTU and LPS, and alterations by JZL184. Data are shown as mean  $\pm$  SD, \*P < 0.05, \*\*P < 0.001

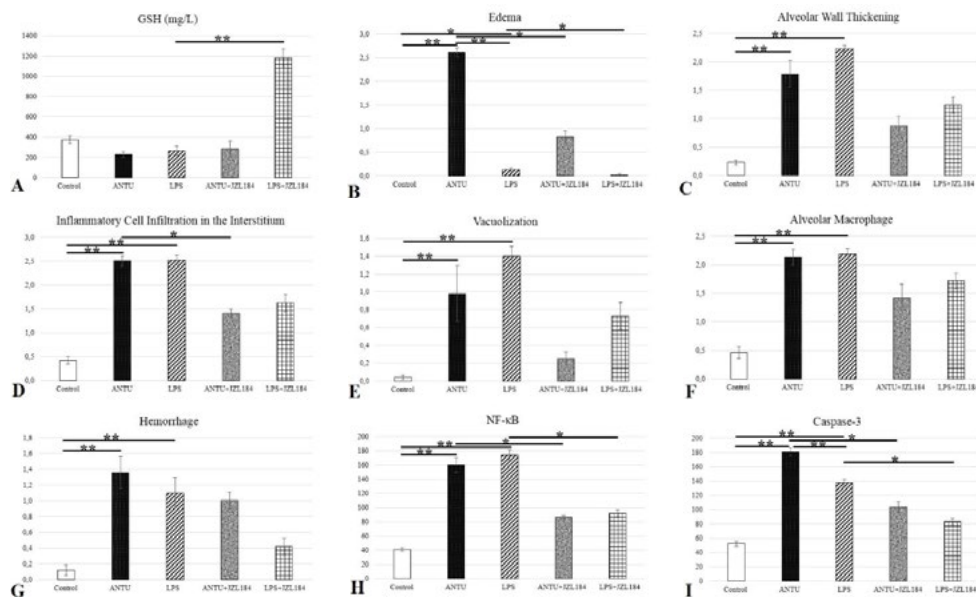


**Figure 3 A:** Results of the biochemical parameter in ARDS induced by ANTU and LPS, and alterations by JZL184. **B-G:** Results of histopathological parameters in ARDS induced by ANTU and LPS, and alterations by JZL184. **H and I:** Results of immunohistochemical parameters in ARDS induced by ANTU and LPS, and alterations by JZL184. Data are shown as mean  $\pm$  SD, \*P < 0.05, \*\*P < 0.001

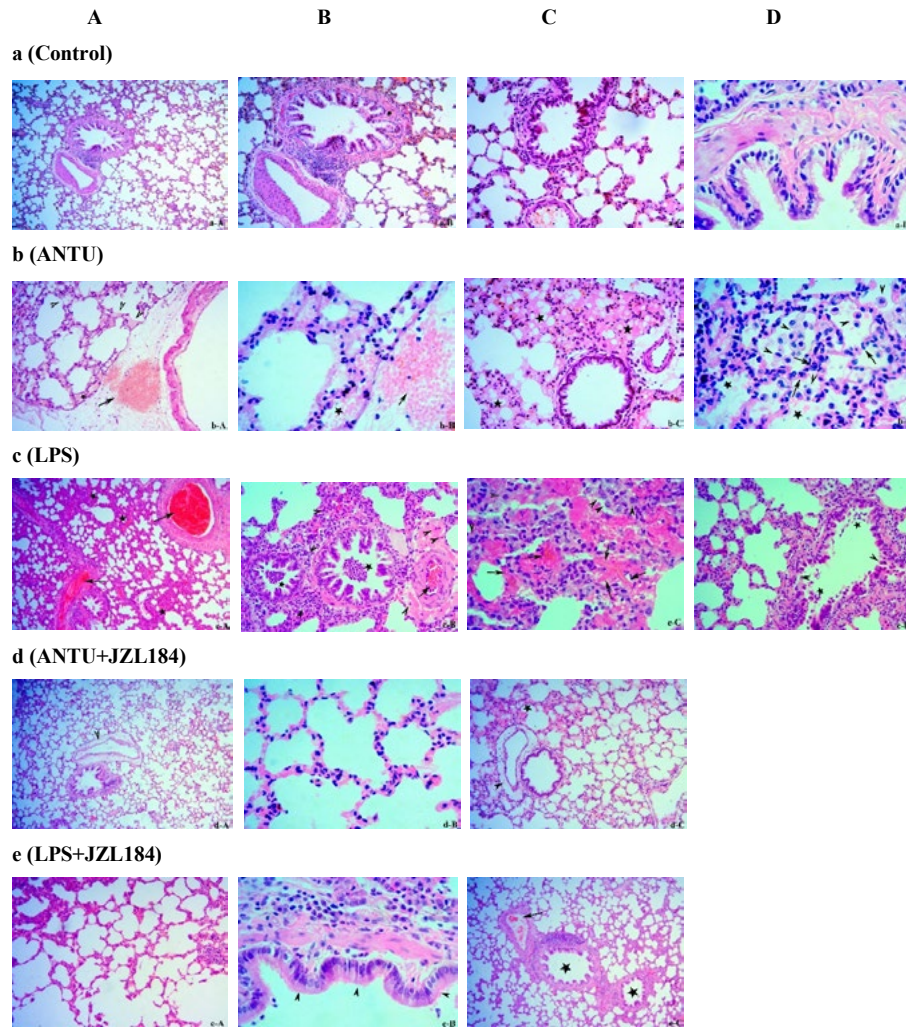


**Figure 4 a-e:** Histopathologic images of normal lung tissues and pathologic lung tissues in ANTU- and LPS-induced ARDS, and alterations by JZL184. a: Normal-appearing lung tissue sections of the control group. Scale bar=A:200  $\mu$ m, B:100  $\mu$ m, C:50  $\mu$ m, D:20  $\mu$ m. b: Lung tissue sections of the ANTU group. Scale bar=A:200  $\mu$ m, B:20  $\mu$ m, C:50  $\mu$ m, D:20  $\mu$ m. c: Lung tissue sections of the LPS group. Scale bar=A:200  $\mu$ m, B:50  $\mu$ m, C:20  $\mu$ m, D:50  $\mu$ m. d: Lung tissue sections of the ANTU+JZL184 treatment group. Scale bar=A:200  $\mu$ m, B:20  $\mu$ m, C:100  $\mu$ m. e: Lung tissue sections of the LPS+JZL184 treatment group. Scale bar=A:100  $\mu$ m, B:20  $\mu$ m, C:200  $\mu$ m

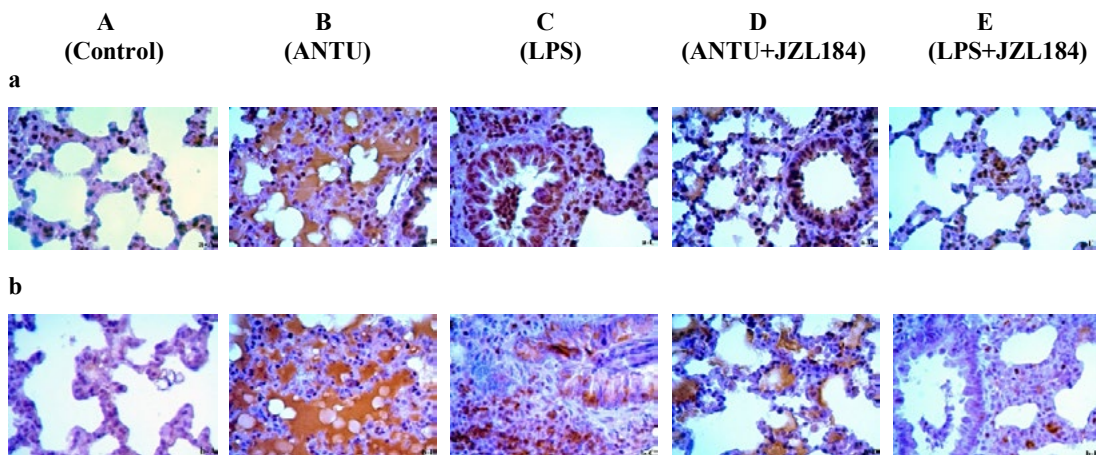


**Figure 5 a, b:** Immunohistochemical staining images to determine NF- $\kappa$ B (a) and caspase-3 (b) expression in all groups. A: Control, B: ANTU, C: LPS, D: ANTU+JZL184, E: LPS+JZL184 (Scale bar: 20  $\mu$ m)

---

#### 4. Discussion

Our study explored the impact of cannabinoids on inflammation, apoptosis, and tissue damage in two ARDS models induced by ANTU (indirect lung injury) and LPS (direct lung injury). We found that JZL184 offers protection against tissue damage, inflammation, and apoptosis in the lung, modulating these processes. Additionally, variations in JZL184's protective effects were noted, aligning with the distinct pathophysiological mechanisms in the two ARDS models.

ARDS, marked by non-cardiac pulmonary edema, increased alveolo-capillary permeability, inflammation, fibrosis, resistant hypoxemia, decreased compliance, reduced functional capacity, and diffuse chest radiography infiltrates, is studied using various animal models [1,2]. In our previous studies, we demonstrated for the first time the roles of endothelin peptides, the L-arginine/nitric oxide (NO) pathway, lipid peroxidation, and inducible nitric oxide synthase (iNOS) expression in ANTU-induced ARDS model and demonstrated that morphine, pentobarbital, thiopental, urethane, and dexmedetomidine can mitigate its effects [16,20-23,28].

Recent findings suggest the endocannabinoid system's role in numerous diseases, positioning it as a potential therapeutic target [5]. The identification of CB<sub>1</sub> and CB<sub>2</sub> receptors, along with their primary ligands anandamide and 2-AG, and related enzymes, has deepened understanding of this system, which is of significant pharmacological interest due to its extensive distribution in mammals and regulatory role in various physiological functions, including immune response and inflammation [29,30]. 2-AG and anandamide are broken down by MAGL and FAAH enzymes, respectively [31]. The endocannabinoid system, involving cannabinoid receptors and various metabolites, modulates immune cell functions and is prevalent in human lungs, with most cell types expressing cannabinoid receptors [32-34]. Research has shown the presence of CB<sub>1</sub> and CB<sub>2</sub> receptors in lung tissues, and many cells can produce endocannabinoids in reaction to inflammatory triggers, though their impact on lung health and disease remains to be fully elucidated. Studies have shown that the CB<sub>2</sub> receptor agonist JWH133 can mitigate lung issues in conditions like RSV infection in human and mice, reduce interstitial lung fibrosis induced by nicotine and ischemia-reperfusion-induced lung damage in mice, suggesting cannabinoids as promising agents for lung disease treatment [35-37].

In our study, the ANTU group exhibited more pronounced edema and perivascular enlargement compared to the LPS group, with non-hemorrhagic, exudative pleural effusion observed only in the ANTU group due to endothelial cell targeting, leading to significant pulmonary edema. Conversely, the LPS group showed limited edema as the primary damage was to the epithelium. Additionally, while the ANTU group had no inflammatory cells in the bronchiolar lumen, the LPS group displayed diffuse inflammatory cell presence, likely due to neutrophil migration following direct LPS administration, with LPS-induced vasodilation contributing to the noticeable congestion in the LPS group.

Lung diseases like ARDS, asthma, and bronchoalveolar dysplasia are linked to unregulated NF-κB activation, with ARDS-related endothelial cell dysfunction being notably influenced by NF-κB [38-40]. In our research, NF-κB staining was predominantly in the alveolar walls in the ANTU group and around the bronchiolar epithelium in the LPS group, indicating that endothelial damage drives ANTU-related injuries, while epithelial damage underlies LPS-induced injuries. The increased NF-κB staining in both injury models highlights the involvement of inflammatory mechanisms in lung pathology.

Apoptosis, a regulated cellular death process initiated through intrinsic or extrinsic pathways, leads to caspase-3 activation—known as the executioner caspase—following caspase-8 or caspase-9 activation [41,42]. Caspase-3 orchestrates apoptosis by targeting various cell components. In our study, like NF-κB, caspase-3 staining was primarily seen in alveolar wall tissues in the ANTU group and near bronchiolar epithelium in the LPS group, indicating apoptosis's role in both endothelial and epithelial damage linked to indirect and direct lung injury mechanisms, respectively. The increased caspase-3 staining in pathology groups points to the significance of apoptotic mechanisms in lung pathology across both injury models.

JZL184 acts by inhibiting MAGL, which breaks down the endocannabinoid 2-AG, thereby elevating 2-AG levels and exhibiting significant immunosuppressive and anti-inflammatory effects [43-45]. Our results corroborate these findings. Similar to a study where a CB<sub>2</sub> agonist (ABK5) reduced hindpaw edema in rats, we observed that JZL184 significantly reduced edema and perivascular dilatation in both injury models, and also lessened pleural effusion in ANTU-induced lung injury, suggesting cannabinoids modulate edema formation mechanisms [46].

JZL184 significantly reduced inflammatory cell presence in the ANTU group's interstitium and the LPS group's bronchiolar lumen, likely due to its effects on cell migration triggered by endothelial injury from ANTU and bronchiolar infiltration from LPS. It also improved desquamation in the LPS group's bronchiolar epithelium with condensed nucleated cells, indicating varied benefits of JZL184 in indirect and direct ARDS models.

JZL184 significantly elevated GSH levels, indicating its potential in reducing oxidative stress by enhancing antioxidant defenses in lung injury. It also diminished NF-κB and caspase-3 staining in both ANTU and LPS groups, with notable reductions in alveolar walls for ANTU+JZL184 and bronchiolar epithelium for LPS+JZL184. These findings suggest that JZL184 modulates inflammatory and apoptotic pathways in lung injury, contributing to its therapeutic effects. The differential modulation in indirect and direct ARDS models points to specific targeting of endothelium and epithelium, respectively.

#### 5. Conclusion

This study demonstrates that inhibiting MAGL offers targeted benefits for ARDS arising from diverse causes, suggesting its

potential as a promising therapeutic strategy for ARDS treatment.

### Funding

This work was supported by the Scientific Research Projects Coordination Unit of Zonguldak Bulent Ecevit University (Project no: 2022-43341027-03).

### Ethical Approval

All experimental procedures described in this study were previously approved by the Ethical Committee of Experimental Animals of Zonguldak Bulent Ecevit University (Protocol No: 2021-25-21/09) and are in accordance with the "Guide for the Care and Use of Laboratory Animals" (US National Institute of Health, revised 1996).

### References

1. Ashbaugh, D., Bigelow, D. B., Petty, T., & Levine, B. (1967). Acute respiratory distress in adults. *The Lancet*, 290(7511), 319-323.
2. Grotberg, J. C., Reynolds, D., & Kraft, B. D. (2023). Management of severe acute respiratory distress syndrome: a primer. *Critical Care*, 27(1), 289.
3. Qadir, N., Sahetya, S., Munshi, L., Summers, C., Abrams, D., Beitler, J., ... & Fan, E. (2024). An update on management of adult patients with acute respiratory distress syndrome: an official American Thoracic Society clinical practice guideline. *American journal of respiratory and critical care medicine*, 209(1), 24-36.
4. Latronico, N., Eikermann, M., Ely, E. W., & Needham, D. M. (2024). Improving management of ARDS: uniting acute management and long-term recovery. *Critical Care*, 28(1), 58.
5. Fraguas-Sánchez, A. I., & Torres-Suárez, A. I. (2018). Medical use of cannabinoids. *Drugs*, 78(16), 1665-1703.
6. Alves, P., Amaral, C., Teixeira, N., & Correia-da-Silva, G. (2020). Cannabis sativa: Much more beyond  $\Delta^9$ -tetrahydrocannabinol. *Pharmacological research*, 157, 104822.
7. Cascorbi, I. (2023). Clinical Pharmacology of Cannabinoid Therapeutics: Drug Interactions and Side Effects. *Clinical Pharmacology & Therapeutics*, 114(5).
8. Cristino, L., Bisogno, T., & Di Marzo, V. (2020). Cannabinoids and the expanded endocannabinoid system in neurological disorders. *Nature Reviews Neurology*, 16(1), 9-29.
9. Bourke, S. L., Schlag, A. K., O'Sullivan, S. E., Nutt, D. J., & Finn, D. P. (2022). Cannabinoids and the endocannabinoid system in fibromyalgia: A review of preclinical and clinical research. *Pharmacology & therapeutics*, 240, 108216.
10. Bilbao, A., & Spanagel, R. (2022). Medical cannabinoids: a pharmacology-based systematic review and meta-analysis for all relevant medical indications. *BMC medicine*, 20(1), 259.
11. Kreitzer, F. R., & Stella, N. (2009). The therapeutic potential of novel cannabinoid receptors. *Pharmacology & therapeutics*, 122(2), 83-96.
12. Di Marzo, V., Bisogno, T., & De Petrocellis, L. (2005). The biosynthesis, fate and pharmacological properties of endocannabinoids. *Cannabinoids*, 147-185.
13. Alger, B. E., & Kim, J. (2011). Supply and demand for endocannabinoids. *Trends in neurosciences*, 34(6), 304-315.
14. Adar, A., Can, E. Y., Elma, Y., Ferah, M. A., Kececi, M., Muderrisoglu, H., ... & Onalan, O. (2022). A new and simple parameter for diagnosis pulmonary edema: Expiratory air humidity. *Heart & Lung*, 52, 165-169.
15. Atalay, F., Yurdakan, G., & Yilmaz-Sipahi, E. (2012). Effect of the endothelin receptor antagonist tezosentan on alpha-naphthylthiourea-induced lung injury in rats. *The Kaohsiung Journal of Medical Sciences*, 28(2), 72-78.
16. Comert, M., Sipahi, E. Y., Ustun, H., Isikdemir, F., Numanoglu, G., Barut, F., ... & Banoglu, Z. N. (2005). Morphine modulates inducible nitric oxide synthase expression and reduces pulmonary oedema induced by  $\alpha$ -naphthylthiourea. *European journal of pharmacology*, 511(2-3), 183-189.
17. Cunningham, A. L., & Hurley, J. V. (1972). Alpha-naphthylthiourea-induced pulmonary oedema in the rat: a topographical and electron-microscope study. *The Journal of pathology*, 106(1), 25-35.
18. Erdem, M. K., Yurdakan, G., & Yilmaz-Sipahi, E. (2014). The effects of ketamine, midazolam and ketamine/xylazine on acute lung injury induced by  $\alpha$ -naphthylthiourea in rats. *Advances in Clinical and Experimental Medicine*, 23(3), 343-351.
19. Kaynar, G., Yurdakan, G., Comert, F., & Yilmaz-Sipahi, E. (2013). Effects of peripheral benzodiazepine receptor ligand Ro5-4864 in four animal models of acute lung injury. *Journal of Surgical Research*, 182(2), 277-284.
20. SIPAHI, E., HODOĞLUGIL, U. G. U. R., ERCAN, Z. S., & TÜRKER, R. K. (1996). Acute effect of endothelin-1 on lung oedema induced by alpha-naphthylthiourea (ANTU). *Pharmacological research*, 33(6), 375-378.
21. Sipahi, E., Hodoğlugil, U., Üstün, H., Zengil, H., Türker, R. K., & Ercan, Z. S. (1997). An unexpected interaction between NG-nitro-l-arginine methyl ester and l-arginine in  $\alpha$ -naphthylthiourea-induced pulmonary oedema in rats. *European journal of pharmacology*, 321(1), 45-51.
22. Sipahi, E., Üstün, H., & Ayoglu, F. N. (2002). Acute effects of pentobarbital, thiopental and urethane on lung oedema induced by alpha-naphthylthiourea (ANTU). *Pharmacological research*, 45(3), 235-239.
23. Sipahi, E. Y., Tekin, I. O., Comert, M., Barut, F., Ustun, H., & Sipahi, T. H. (2004). Oxidized low-density lipoproteins accumulate in rat lung after experimental lung edema induced by alpha-naphthylthiourea (ANTU). *Pharmacological research*, 50(6), 585-591.
24. Khadangi, F., Forgues, A. S., Tremblay-Pitre, S., Dufour-Mailhot, A., Henry, C., Boucher, M., ... & Bossé, Y. (2021). Intranasal versus intratracheal exposure to lipopolysaccharides in a murine model of acute respiratory distress syndrome. *Scientific Reports*, 11(1), 7777.
25. EMİNE, Y. C., KANAT, G., MERYEM, A. F., MURAT, C., & BERRAK, G. The Effects of Cannabinoid System on Acute Lung Injury Induced by Mesenteric Ischemia/Reperfusion in Rats.
26. Suvarna, K. S., Layton, C., & Bancroft, J. D. (2018). *Bancroft's*

*theory and practice of histological techniques*. Elsevier health sciences.

27. Inan, M., Uz, Y. H., Kizilay, G., Topcu-Tarladacalisir, Y., Sapmaz-Metin, M., Akpolat, M., & Aydogdu, N. (2013). Protective effect of sildenafil on liver injury induced by intestinal ischemia/reperfusion. *Journal of pediatric surgery*, 48(8), 1707-1715.
28. Hancı, V., Yurdakan, G., Yurtlu, S., Turan, I. Ö., & Sipahi, E. Y. (2012). Protective effect of dexmedetomidine in a rat model of  $\alpha$ -naphthylthiourea-induced acute lung injury. *Journal of Surgical Research*, 178(1), 424-430.
29. Matsuda, L. A., Lolait, S. J., Brownstein, M. J., Young, A. C., & Bonner, T. I. (1990). Structure of a cannabinoid receptor and functional expression of the cloned cDNA. *Nature*, 346(6284), 561-564.
30. Turcotte, C., Chouinard, F., Lefebvre, J. S., & Flamand, N. (2015). Regulation of inflammation by cannabinoids, the endocannabinoids 2-arachidonoyl-glycerol and arachidonoyl-ethanolamide, and their metabolites. *Journal of Leucocyte Biology*, 97(6), 1049-1070.
31. Costola-de-Souza, C., Ribeiro, A., Ferraz-de-Paula, V., Calefi, A. S., Aloia, T. P. A., Gimenes-Júnior, J. A., ... & Palermo-Neto, J. (2013). Monoacylglycerol lipase (MAGL) inhibition attenuates acute lung injury in mice. *PLoS one*, 8(10), e77706.
32. Galiègue, S., Mary, S., Marchand, J., Dussossoy, D., Carrière, D., Carayon, P., ... & Casellas, P. (1995). Expression of central and peripheral cannabinoid receptors in human immune tissues and leukocyte subpopulations. *European journal of biochemistry*, 232(1), 54-61.
33. Turcotte, C., Blanchet, M. R., Laviolette, M., & Flamand, N. (2016). Impact of cannabis, cannabinoids, and endocannabinoids in the lungs. *Frontiers in pharmacology*, 7, 317.
34. Ribeiro, A., Ferraz-de-Paula, V., Pinheiro, M. L., Vitoretta, L. B., Mariano-Souza, D. P., Quinteiro-Filho, W. M., ... & Palermo-Neto, J. (2012). Cannabidiol, a non-psychotropic plant-derived cannabinoid, decreases inflammation in a murine model of acute lung injury: Role for the adenosine A2A receptor. *European journal of pharmacology*, 678(1-3), 78-85.
35. Tahamtan, A., Samieipoor, Y., Nayeri, F. S., Rahbarimanesh, A. A., Izadi, A., Rashidi-Nezhad, A., ... & Salimi, V. (2018). Effects of cannabinoid receptor type 2 in respiratory syncytial virus infection in human subjects and mice. *Virulence*, 9(1), 217-230.
36. Wawryk-Gawda, E., Chłapek, K., Zarobkiewicz, M. K., Lis-Sochocka, M., Chylińska-Wrzos, P., Boguszewska-Czubara, A., ... & Biała, G. (2018). CB2R agonist prevents nicotine induced lung fibrosis. *Experimental Lung Research*, 44(7), 344-351.
37. Zeng, J., Li, X., Cheng, Y., Ke, B., & Wang, R. (2019). Activation of cannabinoid receptor type 2 reduces lung ischemia reperfusion injury through PI3K/Akt pathway. *International journal of clinical and experimental pathology*, 12(11), 4096.
38. Rieger-Fackeldey, E., & Hentschel, R. (2008). Bronchopulmonary dysplasia and early prophylactic inhaled nitric oxide in preterm infants: current concepts and future research strategies in animal models. *Journal of perinatal medicine*, 36(5), 442-447.
39. Castranova, V. (2004). Signaling pathways controlling the production of inflammatory mediators in response to crystalline silica exposure: role of reactive oxygen/nitrogen species. *Free radical biology and medicine*, 37(7), 916-925.
40. Janssen-Heininger, Y. M., Poynter, M. E., Aesif, S. W., Pantano, C., Ather, J. L., Reynaert, N. L., ... & van der Vliet, A. (2009). Nuclear factor  $\kappa$ B, airway epithelium, and asthma: avenues for redox control. *Proceedings of the American Thoracic Society*, 6(3), 249-255.
41. Wu, H., Che, X., Zheng, Q., Wu, A., Pan, K., Shao, A., ... & Hong, Y. (2014). Caspases: a molecular switch node in the crosstalk between autophagy and apoptosis. *International journal of biological sciences*, 10(9), 1072.
42. Nagata, S. (2018). Apoptosis and clearance of apoptotic cells. *Annual review of immunology*, 36(1), 489-517.
43. Long, J. Z., Li, W., Booker, L., Burston, J. J., Kinsey, S. G., Schlosburg, J. E., ... & Cravatt, B. F. (2009). Selective blockade of 2-arachidonoylglycerol hydrolysis produces cannabinoid behavioral effects. *Nature chemical biology*, 5(1), 37-44.
44. Alhouayek, M., Lambert, D. M., Delzenne, N. M., Cani, P. D., & Muccioli, G. G. (2011). Increasing endogenous 2-arachidonoylglycerol levels counteracts colitis and related systemic inflammation. *The FASEB Journal*, 25(8), 2711-2721.
45. Kerr, D. M., Harhen, B., Okine, B. N., Egan, L. J., Finn, D. P., & Roche, M. (2013). The monoacylglycerol lipase inhibitor JZL 184 attenuates LPS-induced increases in cytokine expression in the rat frontal cortex and plasma: differential mechanisms of action. *British journal of pharmacology*, 169(4), 808-819.
46. Tang, Y., Wolk, B., Britch, S. C., Craft, R. M., & Kendall, D. A. (2021). Anti-inflammatory and antinociceptive effects of the selective cannabinoid CB2 receptor agonist ABK5. *Journal of pharmacological sciences*, 145(4), 319-326.

**Copyright:** ©2024 Emine Yilmaz Can, et al. This is an open-access article distributed under the terms of the Creative Commons Attribution License, which permits unrestricted use, distribution, and reproduction in any medium, provided the original author and source are credited.